PRAMANA
— journal of
physics

© Indian Academy of Sciences

Vol. 80, No. 5
May 2013
pp. 847–854

Effect of the isovector coupling channel on the macroscopic part of the nuclear binding energy

S HADDAD
Physics Department, Atomic Energy Commission of Syria, P.O. Box 6091, Damascus, Syria
E-mail: pscientific@aec.org.sy

MS received 10 June 2012; revised 18 October 2012; accepted 12 December 2012

Abstract. The effect of isovector coupling channel on the macroscopic part of the nuclear binding energy is studied using the relativistic density-dependent Thomas–Fermi approach. The dependency of this effect on the number of neutrons and protons is also studied. The isovector coupling channel leads to increased nuclear binding energy, and this effect increases with the increasing neutron number in the nucleus.

Keywords. Isovector coupling channel; macroscopic part of the nuclear binding energy; relativistic Thomas–Fermi approximation; lead isotopes; $N = 126$ isotones.

PACS Nos 21.10.Dr; 21.30.Fe; 27.80.+w

1. Introduction

The macroscopic part of the nuclear binding energy is evaluated by ignoring the pairing interaction and dropping the shell effects in accordance with the Strutinsky averaging method [1,2]. Its dependency on mass number A and asymmetry parameter $I = (N - Z)/A$, with N and Z being the number of neutrons and protons, is approximated by the liquid-drop formula of the Myers-Swiatecki type [3]:

$$E_{\text{macr}} = -b_{\text{vol}}(1 - K_{\text{vol}}I^2)A + b_{\text{surf}}(1 - K_{\text{surf}}I^2)A^{2/3} + b_{\text{Coul}}Z^2A^{-1/3} - \frac{C_4Z^2}{A}, \quad (1)$$

where b_{vol}, b_{surf}, b_{Coul}, K_{vol}, K_{surf}, and C_4 are the constants of the approximate formula.

The relativistic Brueckner–Hartree–Fock (RBHF) theory is generally accepted as one of the most reliable and feasible microscopic methods for describing the effective interactions in the nuclear medium [4]. In the case of RBHF theory, one gets along with one-boson-exchange potentials, which are only adjusted to the two-nucleon problem. From many-body theoretical standpoint, this scheme contains no adjustable parameters.

DOI: 10.1007/s12043-013-0522-7; ***e*Publication: 17 April 2013**

Theoretical and practical obstacles do not allow for the direct application of the RBHF approach for calculating finite nuclei. Then despite the high complexity of the RBHF approach, the Brueckner scheme is an intermediate density approximation, losing its physical significance at low densities where the Brueckner-independent pair assumption becomes questionable. Therefore, effective interactions with density-dependent meson–nucleon couplings describing the medium dependency of the nuclear interaction have been deduced from the RBHF nuclear matter calculation results of refs [5,6], utilizing the Bonn A potential of ref. [4]. These density-dependent couplings are used for calculating finite nuclei in a relativistic density-dependent Thomas–Fermi (RDTF) approach [7].

The evaluation of nuclear one- and two-body matrix elements shows that the semi-classical Thomas–Fermi (TF) calculations provide the smoothly varying part of these matrix elements, dropping the shell effects in accordance with the Strutinsky averaging method [8], such that the nuclear binding energy resulting from these calculations can be considered as the macroscopic part of the binding energy.

The interest in the isospin dependence of the nuclear force is growing because of the new-generation radioactive beam facilities, such as the Rare Isotope Accelerator in the United States of America, the SPIRAL2 at GANIL/France, and the GSI Facility FAIR in Germany, which produce new data for neutron-rich nuclei.

In this work, the effect of isovector coupling channel of the nucleon–nucleon interaction on the macroscopic part of the binding energy is studied, and the dependency of this effect on the number of neutrons and protons in the nucleus is analysed. The effect of isovector coupling channel of the nuclear interaction on the macroscopic part of the binding energy is determined using the RDTF approach, and the results in the case of both isoscalar and isovector channels are compared with the results in the case of only the isoscalar channel and ignoring the isovector one. The macroscopic part of the nuclear binding energy is determined for spherically symmetric even–even lead isotopes ($Z = 82$), tin isotopes ($Z = 50$), and $N = 126$ isotones with known experimental masses [9], with the aim of analysing the effect of isovector coupling channel on the macroscopic part of the binding energy, and its dependency on the numbers of neutrons and protons in the nucleus. Results are also compared with a modern evaluation of experimental data [10].

Section 2 briefly reviews the effective density-dependent interaction used in this work. Section 3 studies the effect of isovector coupling channel on the macroscopic part of the nuclear binding energy for lead isotopes, and §4 for $N = 126$ isotones. Section 5 considers the effect of isovector coupling channel on the neutron and proton energy levels in ^{208}Pb. Section 6 summarizes the main conclusions.

2. Effective density-dependent interaction

The effective nucleon–nucleon interaction is described in the RDTF by the electromagnetic field between protons and the exchange of four mesons: the isoscalar scalar meson σ, the isoscalar vector meson ω, the isovector scalar meson δ, and the isovector vector meson ρ. Density-dependent coupling parameters for the isoscalar mesons are given by

$$\frac{g_i(\rho)}{g_i(\rho_0)} - 1 = a_i \left(\exp\left[b_i \left(1 - \left(\frac{\rho}{\rho_0} \right)^{1/3} \right) \right] - 1 \right), \quad i = \sigma, \omega, \tag{2}$$

where ρ_0 is the nuclear matter saturation density and a_i, b_i, and $g_i(\rho_0)$ are the coefficients of the density-dependent function $g_i(\rho)$. Density-dependent coupling parameters for the isovector mesons are given by

$$g_i(\rho) = g_i(\rho_0)\exp\left[b_i\left(1-\frac{\rho}{\rho_0}\right)\right], \quad i=\delta,\rho, \tag{3}$$

where b_i and $g_i(\rho_0)$ are the coefficients of the density-dependent function $g_i(\rho)$. The coefficients a_i, b_i, and $g_i(\rho_0)$ ($i=\sigma$, ω) and b_i and $g_i(\rho_0)$ ($i=\delta$, ρ) are adjusted to the outcome of the RBHF calculations of the nucleon self-energy in nuclear matter of refs [5,6] according to

$$\Sigma_{\rm sp}(\rho)+\Sigma_{\rm sn}(\rho) = -2\frac{g_\sigma^2(\rho)}{m_\sigma^2}(\rho_{\rm sp}+\rho_{\rm sn}), \tag{4}$$

$$\Sigma_{\rm sp}(\rho)-\Sigma_{\rm sn}(\rho) = -2\frac{g_\delta^2(\rho)}{m_\delta^2}(\rho_{\rm sp}-\rho_{\rm sn}), \tag{5}$$

$$\Sigma_{0\rm p}(\rho)+\Sigma_{0\rm n}(\rho) = 2\frac{g_\omega^2(\rho)}{m_\omega^2}(\rho_{\rm p}+\rho_{\rm n}), \tag{6}$$

$$\Sigma_{0\rm p}(\rho)-\Sigma_{0\rm n}(\rho) = 2\frac{g_\rho^2(\rho)}{m_\rho^2}(\rho_{\rm p}-\rho_{\rm n}), \tag{7}$$

where $\Sigma_{\rm sp}(\rho)$ denotes the RBHF result for the scalar component of the proton self-energy at density ρ, $\Sigma_{\rm sn}(\rho)$ is the RBHF result for the scalar component of the neutron self-energy at density ρ, $\Sigma_{0\rm p}(\rho)$ is the RBHF result for the vector component of the proton self-energy at density ρ, and $\Sigma_{0\rm n}(\rho)$ is the RBHF result for the vector component of the neutron self-energy at density ρ. m_σ, m_ω, m_δ, and m_ρ are the masses of the σ, ω, δ, and ρ mesons. $\rho_{\rm sp}$ and $\rho_{\rm sn}$ are the scalar proton and neutron densities given by

$$\rho_{\rm sp,sn} = \frac{1}{2\pi^2}\left(M_{\rm p,n}p_{\rm p,n}\varepsilon_{\rm p,n} - M_{\rm p,n}^3\ln\frac{p_{\rm p,n}+\varepsilon_{\rm p,n}}{M_{\rm p,n}}\right), \tag{8}$$

where

$$M_{\rm p,n} = m_N + \Sigma_{\rm sp,sn}, \tag{9}$$

$$p_{\rm p,n}^3 = 3\pi^2\rho_{\rm p,n}, \tag{10}$$

$$\varepsilon_{\rm p,n}^2 = p_{\rm p,n}^2 + M_{\rm p,n}^2. \tag{11}$$

The coefficients of the resulting density-dependent parametrization of the RBHF potential Bonn A [4] are given in table 1. Since the coefficients are adjusted to the outcome of the RBHF calculations of the nucleon self-energy in nuclear matter utilizing the Bonn A potential, the masses m_N, m_σ, m_ω, m_δ, and m_ρ and the saturation density ρ_0 are those of the Bonn A potential.

Table 1. The density-dependent parameter set. m_i is the mass of the meson i. a_i, b_i, and $g_i(\rho_0)$ are the coefficients of parametrization of the density-dependent coupling parameters ($i = \sigma, \omega, \delta, \rho$). $m_N = 938.926$ MeV is the average nucleon mass used by ref. [4] and $\rho_0 = 0.185$ fm^{-3} is the saturation density resulting from the RBHF Bonn A potential [4].

Meson i	σ	ω	δ	ρ
m_i (MeV)	550	782.6	983	769
$g_i(\rho_0)$	9.297	11.269	4.701	2.370
a_i	0.2941	0.3451		
b_i	2.217	2.113	1.223	1.634

The energy density is determined by adding the proton and neutron components:

$$e_{\mathrm{p,n}} = \frac{1}{8\pi^2}\left(5p_{\mathrm{p,n}}^3\varepsilon_{\mathrm{p,n}} - 3p_{\mathrm{p,n}}\varepsilon_{\mathrm{p,n}}^3 + 3M_{\mathrm{p,n}}^4 \ln\frac{p_{\mathrm{p,n}} + \varepsilon_{\mathrm{p,n}}}{M_{\mathrm{p,n}}}\right) + \left(m_N + \frac{1}{2}\Sigma_{\mathrm{sp,sn}}\right)\rho_{\mathrm{sp,sn}} + \frac{1}{2}\Sigma_{\mathrm{0p,0n}}\rho_{\mathrm{p,n}}. \tag{12}$$

The nucleon binding energy B/A is then given as

$$\frac{B}{A} = m_N - \frac{1}{A}\int \mathrm{d}^3r\left(e_{\mathrm{n}} + e_{\mathrm{p}}\right). \tag{13}$$

See refs [7,11], for instance, for a detailed description of the RDTF approach.

The isoscalar coupling channel of the nuclear interaction is represented by the isoscalar scalar meson σ and the isoscalar vector meson ω, while the isovector coupling channel is represented by the isovector scalar meson δ and the isovector vector meson ρ. In order to analyse the role played by the isovector coupling channel, the results obtained using the parametrization of table 1 when all mesons ($\sigma\omega\delta\rho$) included are compared with the results when only isoscalar mesons ($\sigma\omega$) are included.

Two remarks concerning the application of the RDTF approach should be added. First, the density-dependent parameter set in table 1 is adjusted to the outcome of the RBHF calculations of the nucleon self-energy in nuclear matter. Therefore, the parameter set is expected to work at best for heavy nuclei, since nuclear matter conditions are best valid in the interior of heavy nuclei, and second, extending the TF approximation makes the approach applicable also to nuclei close to the drip lines, but the smooth part of the sum of the single particle energies is calculated without using the Strutinsky smearing prescription [12]. This makes the production of the macroscopic part of the binding energy according to the Strutinsky averaging method by extended TF approach questionable.

3. Macroscopic part of the nuclear binding energy in lead isotopes

Figure 1 displays the results for the nucleon binding energy in spherically symmetric even–even lead isotopes with known experimental masses for both cases ($\sigma\omega\delta\rho$) and

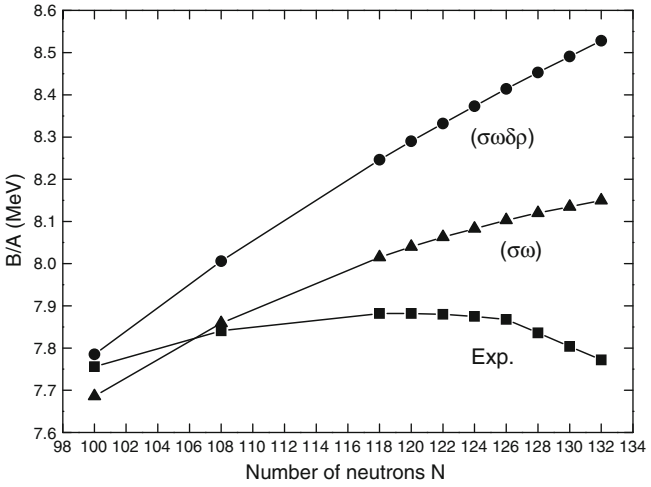

Figure 1. Nucleon binding energy in spherically symmetric even–even lead isotopes with known experimental masses. The figure compares the results for both $\sigma\omega\delta\rho$ and $\sigma\omega$ cases with the results of a modern evaluation of experimental data.

($\sigma\omega$). The results given in ref. [10] for a modern evaluation of experimental data are also displayed in figure 1 for comparison.

Despite the limited agreement with data, which is due to the fact that the RBHF potential is adjusted only to the two-nucleon problem and not to concord with experimental data, figure 1 shows that the inclusion of the isovector coupling channel generally leads to an increase of the value of the nucleon binding energy, and that this increase grows with increasing number of neutrons, i.e., with increasing ratio of neutrons to protons in the nucleus.

Figure 1 displays the nucleon binding energy B/A, which is the total binding energy B divided by A the number of nucleons in the nucleus. The nucleon binding energy is presented instead of the total binding energy to show that the trend of experimental results changes on different sides of the magic number $N = 126$ of neutrons. This is clearly a shell effect, due to the closed-shell configuration at the magic number $N = 126$ of neutrons, and is not produced by macroscopic part calculations ignoring the closed-shell effect at magic neutron or proton numbers.

Despite the first remark at the end of §2, concerning the validity of the use of the RDTF approach for calculating medium and small size nuclei, figure 2 shows that the results of this section are also valid in the case of medium size nuclei of tin isotopes ($Z = 50$).

4. Macroscopic part of the nuclear binding energy in $N = 126$ isotones

Figure 3 displays the results for the nucleon binding energy in spherically symmetric even–even $N = 126$ isotones with known experimental masses for both $\sigma\omega\delta\rho$ and $\sigma\omega$

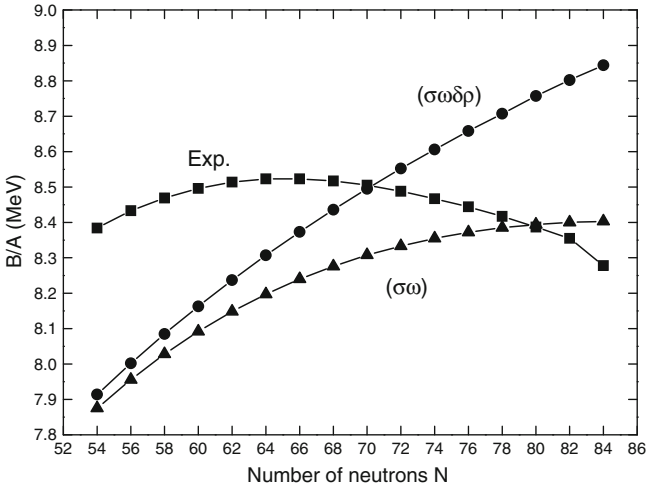

Figure 2. Same as figure 1, but for tin isotopes.

cases. The results given in ref. [10] for a modern evaluation of experimental data are also displayed in figure 3 for comparison.

Figure 3 shows that the inclusion of the isovector coupling channel generally leads to an increase of the value of the nucleon binding energy, and that this increase declines with increasing number of protons, i.e., with decreasing ratio of neutrons to protons in the nucleus, in agreement with the result of the previous section.

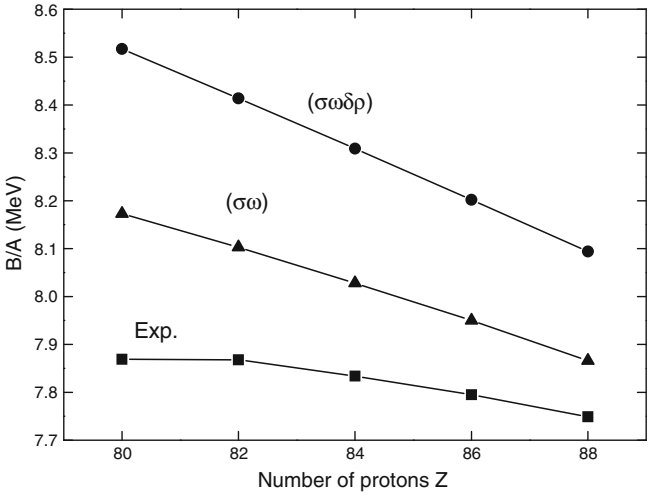

Figure 3. Nucleon binding energy in spherically symmetric even–even $N = 126$ isotones with known experimental masses. The figure compares the results for both $\sigma\omega\delta\rho$ and $\sigma\omega$ cases with the results of a modern evaluation of experimental data.

5. Nucleon energy in the ^{208}Pb nucleus

In order to analyse the effect of isovector coupling channel on the nuclear binding energy, the neutron and proton energy levels in ^{208}Pb nucleus are listed in table 2 for both $\sigma\omega\delta\rho$ and $\sigma\omega$ cases. Experimental levels are from refs [13,14]. One concludes from table 2 that the isovector coupling channel affects neutron and proton energy levels differently. The inclusion of the isovector coupling channel lifts up the proton energy levels and drops down the neutron energy levels, such that the binding energy increases with increasing neutron to proton ratio in the nucleus.

The isovector scalar meson δ leads to a stronger binding between neutrons and a weaker binding between protons when neutron number exceeds proton number (see eq. (5)), while the isovector vector meson ρ leads to a weaker binding between neutrons and a stronger binding between protons in the same case (see eq. (7)). Therefore, one concludes that the effect of isovector scalar meson δ overwhelms the effect of the isovector vector meson ρ, such that the inclusion of the isovector coupling channel results in increasing nuclear binding energy when neutron number exceeds proton number, and that this increase will be more with increasing neutron number in the nucleus, which is the effect noticed in the two previous sections.

Table 2. Neutron and proton energy levels in the ^{208}Pb nucleus in units of MeV. The table compares the results for both $\sigma\omega\delta\rho$ and $\sigma\omega$ cases with experimental data.

Level	$(\sigma\omega\delta\rho)$		$(\sigma\omega)$		Exp.	
	Neutrons	Protons	Neutrons	Protons	Neutrons	Protons
1i 13/2	−8.20		−7.02		−9.01	
3p 1/2	−9.29		−8.00		−7.38	
3p 3/2	−9.99		−8.67		−8.27	
2f 5/2	−10.83		−9.52		−7.95	
2f 7/2	−12.63		−11.30		−9.72	
1h 9/2	−14.44		−13.18		−10.85	
1h 11/2	−17.85	−5.69	−16.63	−7.45		−9.37
3s 1/2	−20.57	−6.28	−19.07	−8.40		−8.03
2d 3/2	−21.46	−7.45	−20.01	−9.47		−8.38
2d 5/2	−22.63	−8.65	−21.19	−10.71		−9.70
1g 7/2	−24.96	−11.68	−23.69	−13.50		−11.43
1g 9/2	−27.44	−14.43	−26.19	−16.26		−15.43
2p 1/2	−32.17	−16.98	−30.65	−19.21		
2p 3/2	−32.78	−17.62	−31.26	−19.87		
1f 5/2	−35.17	−21.06	−33.87	−22.94		
1f 7/2	−36.80	−22.91	−35.52	−24.81		
2s 1/2	−42.89	−26.67	−41.31	−29.08		
1d 3/2	−44.83	−29.80	−43.48	−31.79		
1d 5/2	−45.76	−30.87	−44.40	−32.88		
1p 1/2	−53.69	−37.53	−52.22	−39.70		
1p 3/2	−54.08	−38.00	−52.61	−40.19		
1s 1/2	−61.49	−43.85	−59.82	−46.34		

It should be mentioned here that the neutron and proton energy levels in the ^{208}Pb nucleus are presented in table 2 in order to analyse the effect of isovector coupling channel on the macroscopic part of the binding energy. The ^{208}Pb nucleus is used as an example, but the results on the interplay between the contributions of the δ and ρ mesons are due to the parametrization used, and therefore are expected to be generally valid when neutron number exceeds proton number in the nucleus.

6. Summary

The effect of isovector coupling channel on the macroscopic part of the binding energy was determined using the relativistic density-dependent Thomas–Fermi approach. The dependency of this effect on the number of neutrons and protons in the nucleus is analysed by comparing the results obtained in spherically symmetric even–even lead and tin isotopes and $N = 126$ isotones with known experimental masses.

It is found that the inclusion of the isovector coupling channel generally leads to an increase in the value of the nuclear binding energy, and that this increase grows with increasing number of neutrons and declines with increasing number of protons, such that the effect of isovector coupling channel on the nuclear binding energy sharpens with increasing neutron number in the nucleus. The effect of isovector scalar meson δ overwhelms the effect of isovector vector meson ρ, such that the net effect of the isovector coupling channel is a larger binding energy when neutron number exceeds proton number in the nucleus, and this effect increases with increasing neutron number in the nucleus.

Acknowledgement

The author acknowledges support by the Atomic Energy Commission of Syria.

References

[1] V M Strutinsky, *Nucl. Phys. A* **95**, 420 (1967); *A* **122**, 1 (1968)
[2] M Brack, J Damgård, A S Jensen, H C Pauli, V M Strutinsky and C Y Wong, *Rev. Mod. Phys.* **44**, 320 (1972)
[3] W D Myers and W J Swiatecki, *Nucl. Phys.* **81**, 1 (1966)
[4] R Brockmann and R Machleidt, *Phys. Rev. C* **42**, 1965 (1990)
[5] L Engvik, M Hjorth-Jensen, E Osnes, G Bao and E Østgaard, *Phys. Rev. Lett.* **73**, 2650 (1994)
[6] O Elgaroy, L Engvik, E Osnes, F V De Blasio, M Hjorth-Jensen and G Lazzari, *Phys. Rev. Lett.* **76**, 1994 (1996)
[7] S Haddad, *Acta Phys. Pol. B* **38**, 2121 (2007)
[8] X Viñas, P Schuck, M Farine and M Centelles, *Phys. Rev. C* **67**, 054307 (2003)
[9] P Möller, J R Nix, W D Myers and W J Swiatecki, *At. Data Nucl. Data Tables* **59**, 185 (1995)
[10] G Audi, O Bersillon, J Blachot and A H Wapstra, *Nucl. Phys. A* **729**, 3 (2003)
[11] M K Weigel, S Haddad and F Weber, *J. Phys. G* **17**, 619 (1991)
[12] Z Patyk, A Baran, J F Berger, J Dechargé, J Dobaczewski, P Ring and A Sobiczewski, *Phys. Rev. C* **59**, 704 (1999)
[13] P Grangé and M A Preston, *Nucl. Phys. A* **219**, 266 (1974)
[14] C J Horowitz and B D Serot, *Nucl. Phys. A* **368**, 503 (1981); *A* **399**, 529 (1983)